Analele Universităţii de Vest din Timişoara
Vol. XLIX, 2006
Seria Fizică

FT- IR AND AFM CHARACTERIZATION OF SOL-GEL DERIVED NANOCRYSTALLINE $Zn_2SiO_4:Mn^{2+}$ PHOSPHORS

Corina Enache[1], Cecilia Savii[1], Eugenia Fagadar-Cosma[1], Daniela Dascalu[2], Claudia Ionescu[1]

[1] *Institute of Chemistry Timisoara of Romanian Academy, 24 Mihai Viteazul Blvd, 300223, Timisoara, Romania*
[2] *West University of Timisoara, Faculty of Chemistry, Biology, Geography, 16 Pestalozzi St., 300115, Timisoara, Romania*

Abstract
Manganese activated willemite is an efficient green phosphor. Nanocrystalline powders of manganese doped willemite phosphors, ZnO·1.1SiO2·xMnO ($0.21 \leq x \leq 0.85$), have been obtained via sol-gel route. Beside tetraethoxysilane, water, ethanol, and different catalysts have been employed. In the reaction mixture different inorganic salt solutions, as zinc and manganese (II) sources have been added. The precursor xerogels were successively thermally treated up to 1000ºC, for 180 minutes time soaking. During thermal treatment, the evolution of the system was monitored by using both Thermal Analysis and FT-IR spectroscopy. By using atomic force microscopy (AFM), high-resolution imaging has been obtained, permitting to directly observe the surface morphology. By taking into account the shifts of the Si-O stretching, IR specific features and of the Zn-O stretching vibrational modes, from 1096 cm^{-1} to 940 cm^{-1}, and from 505 cm^{-1} and 455 cm^{-1} to 548 cm^{-1}, respectively, the formation of Si-O-Zn linkage was put in evidence for the samples calcined at 700ºC. Starting from 900ºC thermally treated samples, the arising IR signals corresponding to willemite vibration modes have been observed. AFM pictures revealed an average particle diameter situated in nanometer range.
Keywords: willemite, phosphors, sol-gel method.

1. Introduction

Willemite -α-Zn_2SiO_4 has been identified as a very suitable host matrix for many transition metal and rare earth dopant ions for efficient phosphors. Intensive research has been carried out to improve physical, chemical and photoluminescence properties of willemite phosphors, through new synthetic routes such as the hydrothermal, sol-gel, co-precipitation, combustion synthesis, fume pyrolysis methods and chemical vapor deposition [1]. In this paper, we report the FT-IR and AFM characterization of sol-gel derived nanosized Zn_2SiO_4: Mn phosphor.

2. Method and samples

The powdered, $2ZnO·1,1SiO_2·xMnO$ ($0.21 \leq x \leq 0.85$), willemite phosphors, were synthesized by sol-gel process, starting from: $Si(OC_2H_5)_4$-TEOS, absolute ethanol, water, zinc and manganese salts, and catalysts. Synthesis parameters are presented in Table 1. A and B

series samples are derived from zinc nitrate and acetate, respectively. Xerogels were successively dried at 45, 60 and 105°C, for 10 hours, at each temperature. Further successively thermal treatments were performed at 300, 500, 700, 900 and 1000°C, for 3h.

Table 1. Synthesis parameters of synthesized samples

Sample	EtOH/ TEOS mole ratio	H_2O/ TEOS mole ratio	Catalyst	Catalyst/ TEOS mole ratio	Activator content [mole]	Mn^{2+} precursor	Obs.
A1	15/1	11.2/1	HNO_3	0.02/1	0.085	$Mn(NO_3)_2 \cdot 4H_2O$	
A2	15/1	11.2/1	HNO_3	0.02/1	0.042	$Mn(NO_3)_2 \cdot 4H_2O$	
A3	15/1	11.2/1	HCl	0.02/1	0.085	$MnCl_2 \cdot 4H_2O$	
A4	15/1	12.8/1	NH_4OH	0.55/1	0.085	$MnCl_2 \cdot 4H_2O$	
A5	15/1	20/1	HCl	0.02/1	0.085	$MnCl_2 \cdot 4H_2O$	*
A6	15/1	11.2/1	HCl	0.02/1	0.042	$MnCl_2 \cdot 4H_2O$	
A7	15/1	11.2/1	HCl	0.02/1	0.021	$MnCl_2 \cdot 4H_2O$	
B1	12.5/1	11/1	NH_4OH	1/1	0.085	$MnCl_2 \cdot 4H_2O$	
B2	12.5/1	8/1	CH_3COOH	1.5/1	0.085	$MnCl_2 \cdot 4H_2O$	
B3	12.5/1	19.3/1	NH_4OH	4/1	00.85	$MnCl_2 \cdot 4H_2O$	
B4	50/1	70/1	HCl	0.02/1	0.085	$Mn(CH_3COO)_2 \cdot 2H_2O$	
B5	50/1	70/1	HCl	0.02/1	0.085	$Mn(CH_3COO)_2 \cdot 2H_2O$	**

*2 steps catalysis, in the catalysis second step, it was used NH_4OH until the gelation of sample; mole ratio NH_4OH/TEOS=1.34/1; **Sample with acetylacetone (Acc) mole ratio Acc/TEOS=9/1.

Thermal Analysis was performed with a Mettler-Toledo unit in air atmosphere from 25°C to 1000°C with a heating rate of 10°Cmin^{-1}. FT-IR (JASCO 430 FT-IR, KBr pellets) spectra were carried out, in the 4000-400 cm^{-1} range. AFM images have been obtained.

3. Results and Discussions

Figures 1 and 2 show the thermal curves of A3 and B3 samples respectively. The A3 (60, 140 and 305ºC) endothermic effects were ascribed to zinc nitrate dissolution, water and solvent removal, and organic groups combustion. The exothermic effect (800ºC) is probably due to crystallization [2], [3]. A total weight-loss of 53.63% was registered. Up to 400ºC, the endo- and exothermic peaks of B3 sample can be attributed to the evaporation and combustion of organics. The 790ºC exothermic peak was ascribed to the Zn_2SiO_4 crystalline network formation [4]. Between 30-800ºC the global weight-loss was 38.27%.

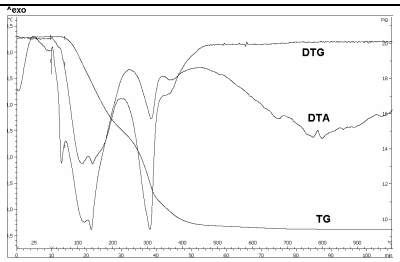

Figure 1. Thermal curves (A3)

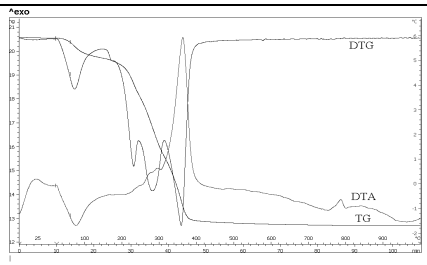

Figure 2. Thermal curves (B3)

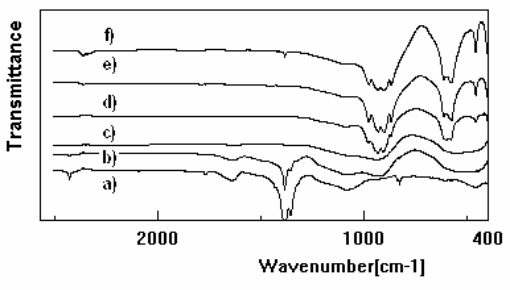

Figure 3. A3 FTIR spectra, 105 ºC (a) 300ºC (b), 500ºC(c), 700ºC(d), 900 (e), 1000ºC (f).

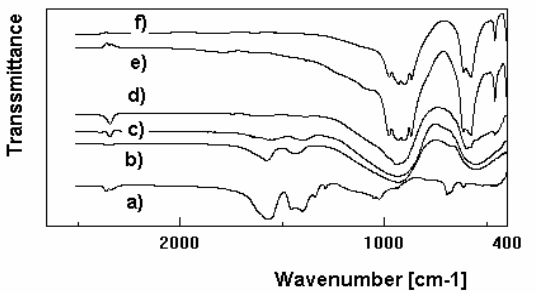

Figure 4. B3 FTIR spectra, 105 ºC (a) 300ºC (b), 500ºC(c), 700ºC(d), 900 (e), 1000ºC (f).

A3 xerogel IR spectrum, Fig.3, shows a 350-750 cm^{-1} broad band, assigned to Zn-O and Si-O-Si bonding [2], [5]. The IR features in 800–850 cm^{-1}, 960-1275 cm^{-1} ranges are also characteristic for Si–O–Si vibration modes. The band situated at 960 cm^{-1} can be attributed to stretching of silanol terminal groups [2]; 830 cm^{-1}, 1385 cm^{-1} and 1355 cm^{-1} peaks corresponding to nitrate ions are also present [6]. As firing temperatures increased, the IR features specific to consuming reactants were gradually diminishing; the 1000 and 1100 cm^{-1} peak width decreases and the peak position shifts towards lower wave numbers, reflecting general trends to the depolimerization of silicate network [7]. The results are consistent with the thermal study. The Si-O-Zn bonds was evidenced by the shift of the Si-O and Zn-O stretching from 1096 cm^{-1} to 940 cm^{-1}, and from 505 cm^{-1} and 455 cm^{-1} to 548 cm^{-1} respectively. IR bonds signals of the sample fired at 1000°C are consistent to vibration modes of willemite: 872 cm^{-1} (ν_1, SiO_4), 978, 934 and 905 cm^{-1} (ν_3, SiO_4), 462, 396 and 380 cm^{-1} (ν_4, SiO_4), 580 cm^{-1} (ν_1, ZnO_4) and 617 and 600 cm^{-1} (ν_3, ZnO_4) [8]. FTIR spectra of B3 xerogel ,Fig. 4, display characteristic bands of zinc acetate such as asymmetric and symmetric stretching of C=O, 1580 and 1420 cm^{-1} respectively, and the 1054 and 1025 cm^{-1} bands belonging to $\nu_{C\text{-}C}$ of acetate [9]. The specific features of Si-O-Si bonds are also present. Starting with of 500°C calcined samples, the IR spectra are quite similar to previous ones.

AFM image of A4 sample, Fig. 6, presents the nanometer range of particle sizes.

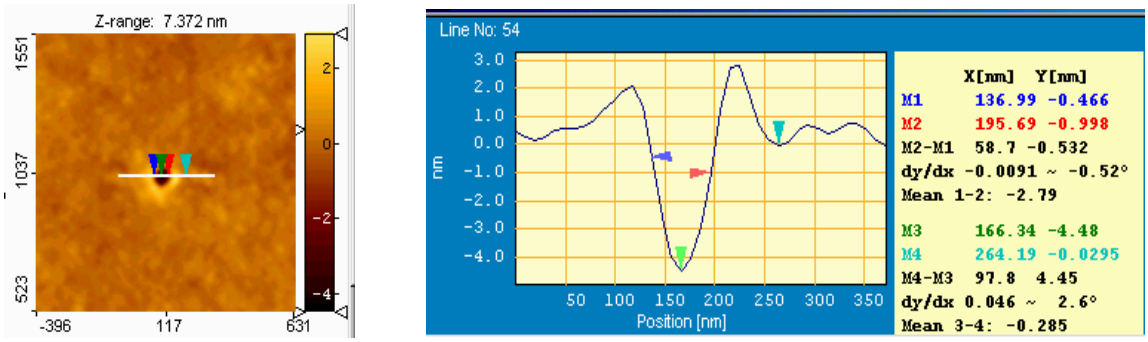

Figure 6. AFM image of A4 sample calcined at 1000ºC

4. Conclusions

The forerunners nature, the thermal parameters and sol-gel employed catalysts effects upon the formation of willemite, it has been studied. By using FTIR analysis, the Si-O-Zn bonds formation (700 ºC) and the IR signals of willemite (900ºC) were put in evidence, in all cases. The results are confirmed by 780ºC exothermic effect on DTA curves. AFM pictures revealed an average particle diameter situated in nanometer range.

Acknowledgements

This work has been partially supported by Research and Ed. Ministry, (MEdC-ANCS) Program, CNCSIS Project Nr.71/223/2006. The authors thank also to Romanian Academy.

References

[1] T. Tani, L. Madler, S. E. Pratsinis, Part. Part. Syst. Charact., 19 (2002) 354-358.

[2] C. J. Brinker, G. W. Scherer, *Sol-Gel Science*, Academic Press, Inc., New York (1990).

[3] Q. Y. Zhang, K. Pita, C. H. Kam, J. Phys. Chem. Solids 64 (2003) 333–338.

[4] H. X. Zhang, C. H. Kam, Y. Zhou, X. Q. Han, S. Buddhudu, Y. L. Lam, C. Y. Chan Thin Solid Films 370 (2000) 50-53.

[5] M. M. Kakazey, V. Melinkova, T. Sreckovic, T. Tomila, J. Mat. Sci., 34(1999)1691-1697.

[6] R. E. Hester, C. W. J. Scaife, J. Chem. Phys., 47 (12) (1967) 5253-5258.

[7] N. Maliavski, O. V. Dushkin, G. Scarinci, Ceram-Silkaty, 45 (2001) 48-54.

[8] C. C. Lin, P. Shen, J. Non-Cryst. Solids, 171 (1994) 281-289.

[9] L. Znaidi, G. J. A. A. Soler Illia, R. Le Guennic, C. Sanchez, A. Kanaev J. Sol-Gel Sci. Technol. 26 (2003) 817–821.